Measurements of a Leaky-Wave Ferrite Isolator

Ahmet Soydan Akyol, *Student Member, IEEE*, and Lionel Edward Davis, *Life Fellow, IEEE*

***Abstract*—A single ferrite/dielectric image line is analyzed using the effective permittivity method adapted for ferrites. E_{pq}^{x} modes are used in association with a transverse bias direction to obtain nonreciprocal behavior. It is shown that the required conditions can be obtained that enable the composite image line to guide in one direction and leak in the other. Thus, the structure behaves as a "leaky-wave isolator." Dispersion diagrams showing this behavior in the frequency range of 14–30 GHz are obtained for a 2 $\times$ 2 mm^2 ferrite (type TT1-390) rod with adjacent dielectric loading with $\varepsilon r = 10$. The structure is built and the bias is applied externally in a direction transverse to and in the plane of the direction of propagation. The required modes are excited and probed by semirigid coaxial cables mounted on vernier mechanisms. The S-parameters indicating the nonreciprocal behavior in the frequency range expected are shown.**

***Index Terms*—Ferrite, image guide, isolator, leaky wave, nonreciprocity, transverse magnetization.**

I. Introduction

THE increased interest in millimeter-wave systems presents challenges in the design of ferrite components. Assuming that all other ferrite-related parameters remain constant, an inherent problem is the reduction in gyrotropy as the signal frequency is increased, i.e., the off-diagonal component of the ferrite permeability approaches zero as the frequency is increased well above ferrimagnetic resonance. A second problem is the increase in conductor loss as the frequency is increased. Therefore, it is helpful if a component can be devised that minimizes the use of the conductor and requires only weak gyrotropy. This paper describes a new type of isolator that combines these features, i.e., a nonreciprocal ferrite image guide. It is the ferrite equivalent of a dielectric image guide, but it guides in one direction and leaks in the other direction. An approximate analysis of this structure has been presented previously [1] and a similar concept for lightwave components has also been proposed [2]. A dielectric image guide can be visualized as half the cross section of an optical fiber, on a conducting ground plane, scaled up to millimetric wavelengths. Dielectric waveguides have been described by a number of authors [3]–[6], and McLevige *et al.* [6] also considered the insulated image line, as well as the grounded image line. The "effective permittivity" method is used in [7] and also used in this paper, but is modified to analyze this paper's structure that includes ferrites.

Manuscript received April 29, 2002; revised October 27, 2002.

A. S. Akyol was with the Department of Electrical and Electronic Engineering, University of Manchester Institute of Science and Technology, Manchester M60 1QD, U.K. He is now with ASELSAN A.S., Yenimahalle, Ankara 06172, Turkey (e-mail: sakyol@mst.aselsan.com.tr).

L. E. Davis is with the Electromagnetics Centre, Department of Electrical Engineering and Electronics, University of Manchester Institute of Science and Technology, Manchester M60 1QD, U.K. (e-mail: l.davis@umist.ac.uk).

Digital Object Identifier 10.1109/TMTT.2003.810148

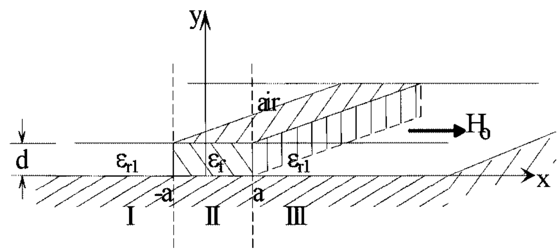

Fig. 1. Ferrite image guide structure (wave propagation in z-direction).

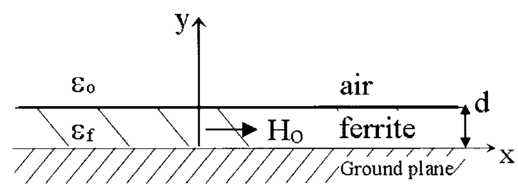

Fig. 2. Infinite ferrite slab on a ground plane (wave propagation in the z-direction).

Ferrite image guides have been investigated by several authors [8]–[10], principally in the context of ferrite-controlled coupling between dielectric image guides. In [7], based on earlier analysis in [11], an isolator was described based on nonreciprocal coupling between two dielectric image guides. The coupling was through a transversely magnetized ferrite layer placed over the image guides. In [9], the use of a ferrite with the bias field applied in the x-, y-, or z-direction was investigated to control the coupling between two dielectric image guides. Nonreciprocal behavior was found with all three orientations, but large bias fields were found to be necessary. The analytical approach in our paper and in those cited above is similar, but this study investigates the properties of a single guiding structure, does not involve coupling between two structures, and selects the modes and bias direction required to enhance the nonreciprocal behavior.

II. Ferrite Structure

The ferrite image guide is shown in Fig. 1. It consists of a rectangular ferrite rod (relative permittivity ε_f, width $2a$, and height d) on a metallic ground plane with identical dielectric slabs on both sides extending to infinity. The rod and slabs have the same height, and the region above them has a low permittivity, typically air. The dielectric slabs have a relative permittivity ε_{r1}, where $\varepsilon_{r1} < \varepsilon_f$. Propagation is in the z-direction and the ferrite is biased in the plane of the structure and transverse to the direction of propagation. In the first stage of the "effective permittivity" method, each of the regions I–III ($=$ I) shown in Fig. 1 is considered separately as a horizontal slab (thickness d) of infinite extent on a ground plane, as shown in Fig. 2 and

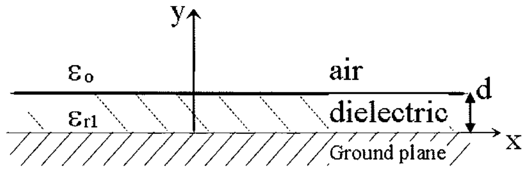

Fig. 3. Infinite dielectric slab on a ground-plane plane (wave propagation in the z-direction).

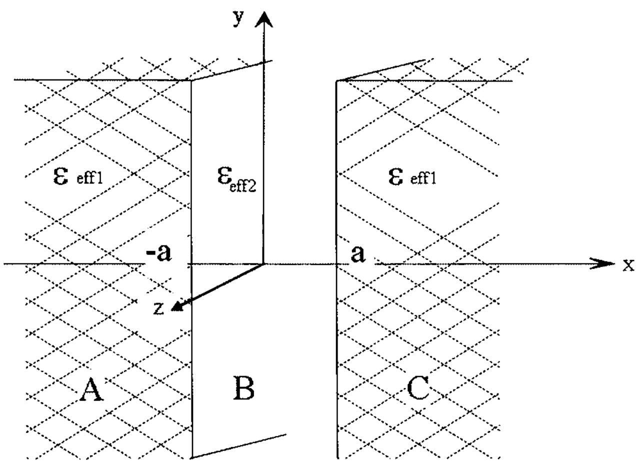

Fig. 4. Hypothetical model to approximate the propagation constants of the original structure (wave propagation in the z-direction).

Fig. 3. These slabs will support TE or TM modes that are dependent on the dimensions, material parameters, and frequency. The propagation constants of infinite slabs in these new models can be found by matching tangential electric and magnetic fields at the boundaries. The TE and TM solutions have E-field orientations that are related to the E^x_{pq} and E^y_{pq} modes of the initial image guide. However, the TE modes are required for this application to ensure that the principal RF magnetic-field components are in the yz-plane, i.e., perpendicular to the bias direction ($\partial/\partial x = 0$). Each region can then be replaced by a homogeneous region, this time infinite in the y-direction ($\partial/\partial y = 0$), and having effective dielectric constants that are defined analytically by using propagation constants of structures of Figs. 2 and 3. The final structure to analyze is that shown in Fig. 4. The propagation constants of the original structure can be approximated using this new hypothetical model. With this orientation of the layers, the TM modes are required for this application so that, again, the RF magnetic-field component is in the yz-plane and the overall solutions correspond to E^x_{pq} modes of the original structure.

If $\varepsilon_{\text{eff2}} > \varepsilon_{\text{eff1}}$, the central rib will guide a wave, and if $\varepsilon_{\text{eff2}} < \varepsilon_{\text{eff1}}$, it will not. The novel feature of this structure is that this inequality can be controlled because, due to the transverse bias field, the TE modes of the conductor-backed infinite ferrite slab, shown in Fig. 2, exhibits nonreciprocal field displacement. [12]. This means that $\beta^+ \neq \beta^-$ and, consequently, the effective permittivity $\varepsilon^+_{\text{eff2}} \neq \varepsilon^-_{\text{eff2}}$. Thus, it becomes possible to create the required conditions to guide waves one way, but not the other. Such a device is a "radiative or leaky-wave isolator" and it has not been observed previously in the microwave literature.

III. Derivation of Propagation Constants

MATLAB m files were written for all three structures and the transcendental equations related to each case were solved numerically. The ferrite is type TT1-390 with saturation magnetization of $4\pi M_s = 2150$ G and $\varepsilon_f = 12.7$. It is biased in the $\pm x$ direction with $H_o = 500$ Oe. All losses are ignored. The thickness $d = 2$ mm and the half-width $a = 4$ mm. The dielectric constant of the dielectric layers is $\varepsilon_{r1} = 10$. We will first begin with Fig. 2, considering solutions where fields are guided by the ferrite region and field components can be derived from a magnetic potential ϕ_h as follows:

$$\phi_h = e_x = \begin{Bmatrix} A_1 e^{-k_1(y-d)}, & y \geq d \\ A \sin k_2 y, & d > y \geq 0 \end{Bmatrix} \tag{1}$$

$$\begin{aligned} k_1^2 &= k_z^2 - k_o^2 \\ k_2^2 &= \varepsilon_f \mu_{\text{eff}} k_o^2 - k_z^2 \end{aligned} \tag{2}$$

$$\begin{aligned} h_y &= \frac{k_z e_x - \dfrac{\kappa}{\mu}\dfrac{\partial e_x}{\partial y}}{\omega \mu_{\text{eff}}} \\ h_z &= \frac{\dfrac{\partial e_x}{\partial y} - \dfrac{\kappa}{\mu} k_z e_x}{j\omega \mu_{\text{eff}}} \end{aligned} \tag{3}$$

where $\mu_{\text{eff}} = (\mu^2 - \kappa^2)/\mu$ is the effective permeability, k_z is the propagation constant, and $k_o = \omega^2 \mu_o \varepsilon_o$. The definitions of all the parameters appearing in the field expressions are well known and can be found in [13]. The effective dielectric constant of the overall structure is given by

$$\varepsilon_{\text{eff2}} = \varepsilon_f \mu_{\text{eff}} - (k_2/k_o)^2. \tag{4}$$

Similarly, for the structure of Fig. 3, (1)–(3) can be modified for the dielectric slab and effective dielectric constants can be obtained from propagation constants by applying the boundary conditions to the following field expressions:

$$\phi_h = \begin{Bmatrix} A_2 e^{-k'_a(y-d)}, & y \geq d \\ A_1 \sin k'_2 y, & d > y \geq 0 \end{Bmatrix} \tag{5}$$

$$\begin{aligned} k_2'^2 &= \varepsilon_{r1} k_o^2 - k_z'^2 \\ k_a'^2 &= k_z'^2 - k_o^2 \end{aligned} \tag{6}$$

$$e_x = \omega \mu_o k'_z \phi_h \tag{7}$$

$$h_z = -jk'_z \partial\phi_h/\partial y \tag{8}$$

$$\varepsilon_{\text{eff1}} = \varepsilon_{r1} - (k'_2/k_o)^2. \tag{9}$$

It is well known that TE modes in grounded ferrite slabs biased as shown in Fig. 2 exhibit nonreciprocal behavior [12]. Nonreciprocity is observed as having different propagation constants and different field distributions for positive and negative going waves. As the propagation constants differ with respect to the direction of propagation (this is same as changing the bias direction), it is possible to obtain two different effective dielectric constants for the two different directions. Table I shows the propagation constants with respect to frequency obtained for the structures of Fig. 2 and Fig. 3, in which $d = 2$ mm. There are two different propagation constants for two bias directions for

TABLE I
PROPAGATION (BETA RADIANS PER METER) AND EFFECTIVE DIELECTRIC CONSTANTS OF STRUCTURES IN FIGS. 2 AND 3

freq (GHz)	beta (+)	beta (-)	beta (diel)	Eeff1	Eeff2(+)	Eeff2(-)
14	293.2	419.9	326.8	1.24	0.99	2.05
15	355.0	521.3	393.3	1.56	1.27	2.75
16	445.6	618	467.9	1.94	1.76	3.4
17	543.5	711.2	546.2	2.35	2.32	3.98
18	643.4	862.1	626.3	2.75	2.91	4.52
20	847.7	979.5	787.5	3.53	4.04	5.46
21	940.8	1066.7	867.9	3.89	4.57	5.88
23	1133.1	1239.2	1027.3	4.54	5.53	6.61
25	1320.4	1409.8	1184.6	5.18	6.35	7.24
30	1770.3	1829.6	1568.9	6.23	7.93	8.47

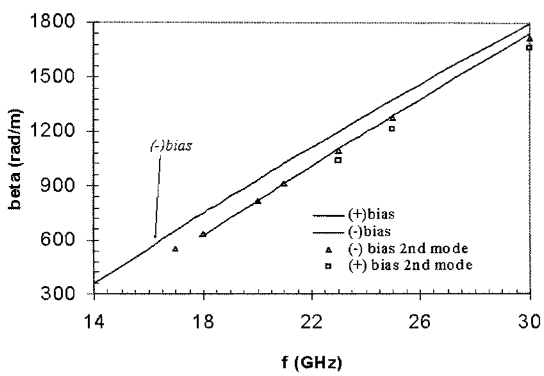

Fig. 5. Approximate propagation constants of the original structure showing isolation over a frequency range of 14–18 GHz. ($a = 4$ mm, $d = 2$ mm, $H_o = 500$ Oe, $\varepsilon_{r1} = 10$) (from Table II).

the infinite ferrite slab [denoted beta (+) and beta (−)]. The fourth column, beta (diel), on the other hand, shows the propagation constants of the dielectric slab. It can be seen that even though $\varepsilon_{\rm eff2}$ (−) is always greater than $\varepsilon_{\rm eff1}$, $\varepsilon_{\rm eff2}$ (+) is smaller at lower frequencies and greater at higher frequencies due to the difference in the propagation constants of the ferrite slab with different bias directions. Thus, for the structure shown in Fig. 4, in which the effective constants will be used, it becomes possible to create the required conditions to guide the waves in one direction (where $\varepsilon_{\rm eff2} > \varepsilon_{\rm eff1}$) and not in the other (where $\varepsilon_{\rm eff2} < \varepsilon_{\rm eff1}$). If region II in Fig. 2 were a simple dielectric with the same dielectric constant of the ferrite used, there would always be reciprocal propagation in both directions. However, due to the nonreciprocal behavior, the ferrite slab acts as if it has a smaller dielectric constant in one direction and a higher value in the other. This is the key idea behind the proposal for a new type of isolator. Having determined the effective dielectric constants, the field solutions for Fig. 4 can be written assuming a sinusoidal variation in Region B and exponential decays in Regions A and C. Analysis is not given here due to lack of space. Fig. 5 shows a plot of propagation constants of the structure of Fig. 4, which approximates the propagation constants of the original structure. It can be seen that the dispersion curves for two different propagation directions do not start from the same frequency. The propagation constants are also tabulated in Table II.

Fig. 5 shows that it is possible to have propagation in one direction and not in the other for approximately 4 GHz (from 14 to 18 GHz). This numerical example is only a preliminary study and it is possible to improve the bandwidth of the isolation by changing either the bias strength or the $\varepsilon_f/\varepsilon_{r1}$ ratio [1]. It is also possible to eliminate the higher order modes by changing the width of the center rib. Fig. 6 shows a plot of the propagation constants of the same structure where the half-width of the central rib is decreased to 1 mm. The propagation constants are tabulated in Table III.

IV. EXPERIMENTAL STRUCTURE

The dc magnetic field required to bias the ferrite was obtained using an electromagnet with circular pole pieces and a current-reversal switch (Fig. 7). In order to hold the isolator structure between the poles of the magnet, an aluminum case was designed as a support unit. The inner bottom surface of the case was used as the ground plane of the image guide structure (see Fig. 8). The dielectric waveguides and ferrite rod were located on this surface. The dielectrics were fitted on the supporting unit by nylon screws and, in order to fit the ferrite rod in the middle, the dielectric portions were made movable. This was done by drilling slots across the dielectric with the same size of the diameter of the screws. The sidewalls of the support unit were designed to provide a rigid body to hold the device between the movable poles. The inner width of the supporting case was chosen large enough (32 mm) to accommodate reasonably wide portions of dielectric slabs. Some additional gap was left between the dielectric and the walls to allow absorbing material to be inserted. The model used in the isolator structure assumes infinite dielectric slabs on both sides of the ferrite.

The dielectric slabs were obtained from a microwave laminate. The dielectric material is a PTFE ceramic with a relative permittivity of $\varepsilon_r = 10.2 \pm 0.250$. The thickness of the dielectric is 0.075 in (1.905 mm). Two pieces of 10 $\times$ 100 mm (width $\times$ length) laminates were cut by mechanical techniques and then the slots were opened for the screws. The cutting and drilling was done while the copper cladding was on because the copper layers increased the rigidity of the whole material. The copper foil on both sides was then removed by photolithographic techniques. The copper on one side could have been left on to serve as a more uniform ground layer, however, it was easier to remove both sides by immersing the whole piece. According to the model, the required thickness of the dielectric was 2 mm, however, the thickness of the dielectric without the metal cladding was 1.905 mm. The central rod was a TT1-390 magnesium ferrite, with saturation magnetization of $4\pi M_s = 2150 \pm 5\%$ G, a linewidth of $\Delta H = 540 \pm 20\%$ Oe, and a relative permittivity of $\varepsilon_f = 12.7 \pm 5\%$. The rod was 2 $\times$ 2 mm (height $\times$ width) with a length of 100 mm. The ferrite parts were supplied with ground surfaces and discontinuities due to air gaps were minimized by pushing the dielectrics toward the center rod. To excite and probe the required mode E_{11}^x, the RF magnetic field of coaxial-cable probes were used with the outer conductor stripped off and the inner conductor bent to form a quarter of a circle. To permit adjustment, the probes were positioned using two three-dimensional vernier mechanisms. The designed mechanisms were fitted on top of the aluminum support unit sidewalls. Using the mechanism, a probe can be pushed forward or pulled backward or moved up or down to obtain

TABLE II
APPROXIMATE PROPAGATION CONSTANTS OF THE ORIGINAL STRUCTURE FOUND USING THE HYPOTHETICAL MODEL SHOWN IN FIG. 4 ($a = 4$ mm, $Ho = 500$ Oe, $\varepsilon r1 = 10$)

f (GHz)	β rad/m (+) bias 1st mode	β rad/m (+) bias 2nd mode	β rad/m (+) bias 3rd mode	β rad/m (-) bias 1st mode	β rad/m (-) bias 2nd mode	β rad/m (-) bias 3rd mode
14	x	x	x	360.49	x	x
15	x	x	x	455.78	x	x
16	x	x	x	554.83	x	x
17	x	x	x	652.36	549.88	x
18	630.2	x	x	747.63	637.23	x
20	815.43	x	x	932.37	819.21	x
21	910.8	x	x	1022.55	911.21	x
23	1101.31	1033.47	x	1199.85	1094.23	x
25	1289	1210.91	x	1374.07	1274.83	x
30	1742.25	1662.98	1570.95	1800.25	1715.2	1597.23

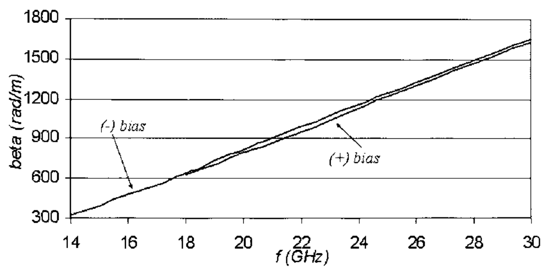

Fig. 6. Elimination of higher order modes up to 30 GHz by reducing ferrite width ($a = 1$ mm, $d = 2$ mm, $H_o = 500$ Oe, $\varepsilon_{r1} = 10$).

TABLE III
APPROXIMATE PROPAGATION CONSTANTS OF THE ORIGINAL STRUCTURE FOUND USING THE HYPOTHETICAL MODEL SHOWN IN FIG. 4 ($a = 1$ mm, $Ho = 500$ Oe, $\varepsilon r1 = 10$)

freq (GHz)	beta (+) bias	beta (-) bias
14		329.5
15		398.9
16		477.1
17		559.6
18	626.6	644.2
20	791.1	815.4
21	874.4	901.1
23	1042	1071.9
25	1215.6	1246.5
30	1630.9	1660.8

a best match for both launching the waves from the first port and probing them from the second. It also provided a very easy method to access the isolator, which was positioned between the pole pieces of the electromagnet where access was obstructed by the large electromagnet pieces. The open ends of the isolator behind the coaxial probe positions were terminated by microwave absorbers to reduce reflections from the end discontinuities. Fig. 8 shows the ferrite image guide fitted on a metal ground plane. The S-parameters of the structure were measured using an HP 8720 vector network analyzer and the input and output ports were extended by extra lengths of RG405 semirigid coaxial cable. These extensions were connected to the probes that were used to launch the waves into the isolator and sample the field from the isolator via male and female subminiature A (SMA) connectors and adapters. A full two-port calibration was done at point X and Y (see Fig. 7). Therefore, the results include the losses in the excitation and sampling probes, and the coupling between the probes and the guiding structure was not calculated. The fundamental aim of this experiment was to determine whether the nonreciprocal behavior occurred within the calculated leaky-wave frequency range.

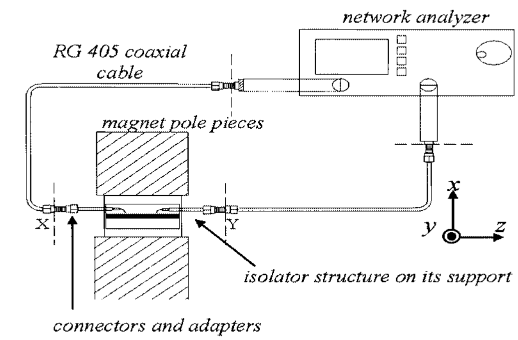

Fig. 7. Schematic diagram of the experimental setup to measure the S-parameters.

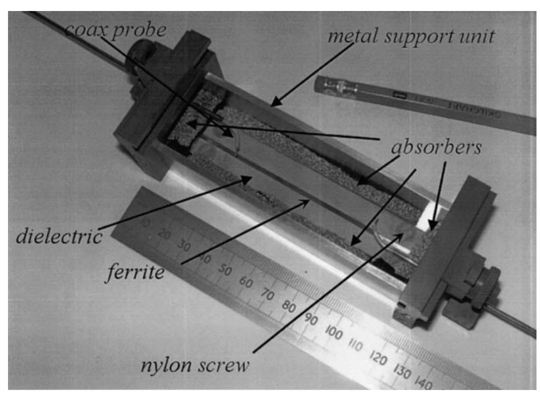

Fig. 8. Ferrite image guide isolator with its support unit.

V. RESULTS AND DISCUSSION

Fig. 9 shows the S-parameters from 14 to 16 GHz, measured between points X and Y of Fig. 7, when the structure is positioned between the magnet poles, but not biased. The tips of the coaxial cables are 25 mm apart. $S11$ and $S22$ are approximately -7 to -10 dB within the frequency range, and the insertion loss is around -28 dB. These S-parameters will be taken as a reference for the other measurements so that the insertion loss of the isolator can be estimated. Note that $S21$ is almost the same as $S12$ when there is no external bias. i.e., the device is reciprocal.

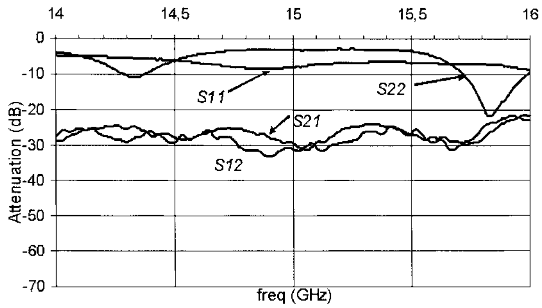

Fig. 9. S-parameters of the isolator without external bias.

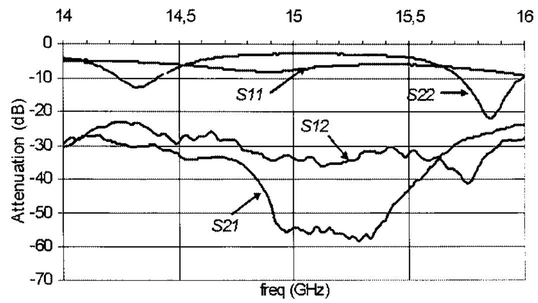

Fig. 10. S-parameters when the isolator structure is biased in the positive direction.

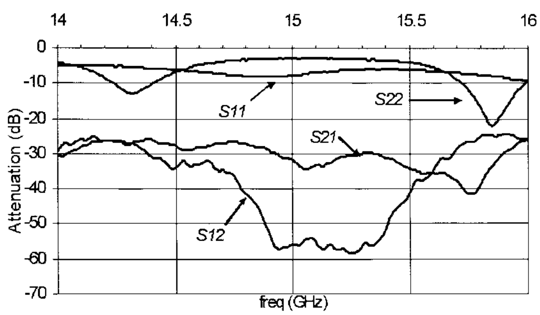

Fig. 11. S-parameters when the isolator structure is biased in the negative direction.

Fig. 10 shows the S-parameters when the isolator is biased in the positive direction. It can be seen that $S12 \neq S21$ and the differential isolation is approximately -20 dB for approximately 1 GHz. The graph shows that there is propagation in one direction and comparatively no guidance in the other. Fig. 11 shows the S-parameters when the direction of bias is reversed. Changing the direction of bias is equivalent to changing the direction of propagation. In this case, there is a -30-dB drop in S_{12}, whereas S_{21} stays the same. Fig. 12 shows the difference in S_{12} and S_{21} between the positive bias and no bias cases. Fig. 13 shows the difference in S_{12} and S_{21} between negative-bias and no-bias cases.

The following observations regarding these first results can be made. The coaxial probe structure was chosen for convenience of fabrication and ease of movement with respect to the ferrite rod and electromagnet. However, the poor launching efficiency degraded the true performance of the isolator and, therefore, alternative techniques for coupling to the ferrite image guide need to be explored, e.g., the use of apertures or direct waveguide feeds. Also, the required level of dc bias needs to

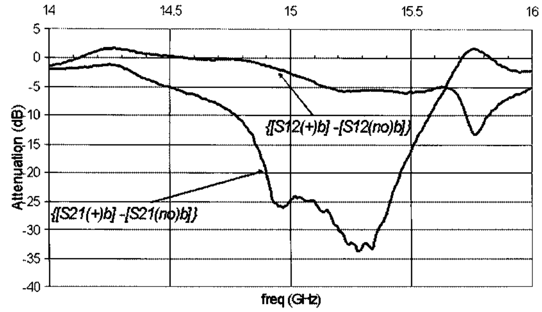

Fig. 12. Difference of S_{12} and S_{21} between the $(+)$ bias case and (no) bias case.

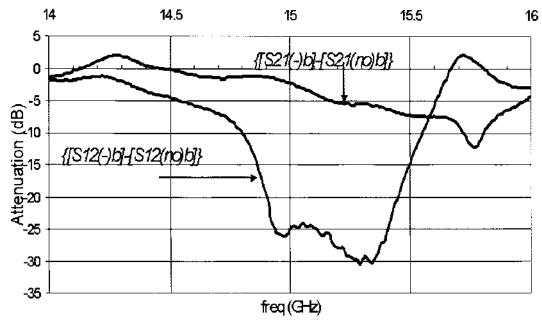

Fig. 13. Difference of S_{12} and S_{21} between the $(-)$ bias case and (no) bias case.

be explored further with more compact measurement jig. It was found that the applied static field, measured at a point corresponding to the center of the ferrite rod (in the absence of the rod), $H_a = 3000$–4000 Oe. With a ferrite saturation magnetization $4\pi M_s = 2150$ G and a transverse demagnetization factor $N_t \approx 0.5$, it was estimated that, at the center point, the internal field $H_i = 2000$–3000 Oe. This is less than would be required for resonance, but is higher than that used in the approximate design model. (A uniform value of $H_i = 500$ Oe was used in the "adapted effective dielectric constant method.") The transverse field applied across the rod was unavoidably nonuniform along its length, but the shape and frequency range and the levels of insertion and isolation losses shown in Figs. 9–13 were relatively insensitive to variations in the applied field within the range of H_a given above. The performance was found to be sensitive to the positioning of the absorbing materials at the sides and the ends of the ferrite/dielectric image guide. This was expected since it is a radiative isolator, and further analysis of the field distribution and experimental work is required to optimize the positioning and shaping of the lossy regions to minimize the insertion loss of the forward wave and provide sufficient isolation of the reverse wave.

VI. Conclusions

It has been shown that, by selecting the correct modes and bias direction, a method exists to obtain a leaky-wave ferrite image guide isolator. With an appropriate choice of constitutive parameters, dimensions and bias strength nonreciprocal leaky-wave behavior was predicted over a frequency range of 14–18 GHz with higher order modes suppressed up to 30 GHz. It is predicted that such structures need a low bias field and, therefore, they would overcome one of the difficulties of building conventional transverse-field isolators at millimetric wavelengths, i.e., the need for large applied fields to overcome the weak gyrotropy. It also minimizes the use of metal conductors and thereby reduces conductor loss. A numerical technique, used to obtain the propagation constants of dielectric image guides, known as the effective dielectric-constant method, has been adapted to obtain the propagation constants of the ferrite/dielectric structure. An analysis of ferrite slabs and metal-backed ferrite slabs was used to find the required frequency range for possible nonreciprocal behavior. The measured S-parameters indicated a differential isolation of approximately 20 dB and an insertion loss of approximately 5 dB at 15–15.5 GHz and, thus, the proof-of-principle experiment was successful in demonstrating nonreciprocal behavior within the frequency range expected.

ACKNOWLEDGMENT

The authors would like to thank Microwave Applications Group, Santa Maria, CA, and the Rogers Corporation, Chandler, AZ, who supplied the ferrite parts and the dielectric materials, respectively, and R. Dunkley, the University of Manchester Institute of Science and Technology (UMIST), Manchester, U.K., for the fabrication of the isolator support jig.

REFERENCES

[1] A. S. Akyol and L. E. Davis, "A novel nonreciprocal ferrite image guide," in *IEEE MTT-S Int. Microwave Symp. Dig.*, vol. 2, Phoenix, AZ, June 2001, pp. 1179–1182.

[2] K. Xie and L. E. Davis, "Radiative optical isolator and circulator," *J. Lightwave Technol.*, vol. 19, pp. 1028–1035, July 2001.

[3] E. A. J. Marcatili, "Dielectric rectangular waveguide and directional coupler for integrated optics," *Bell Syst. Tech. J.*, vol. 48, pp. 2079–2102, Sept. 1969.

[4] J. E. Goell, "A circular-harmonic computer analysis of rectangular dielectric waveguides," *Bell Syst. Tech. J.*, vol. 48, pp. 2133–2160, Sept. 1969.

[5] H. Jacobs and M. M. Chrepta, "Electronic phase shifter for millimeter-wave semiconductor dielectric integrated circuits," *IEEE Trans. Microwave Theory Tech.*, vol. MTT-22, pp. 411–417, Apr. 1974.

[6] W. V. McLevige, T. Itoh, and R. Mittra, "New waveguide structures for millimeter-wave and optical integrated circuits," *IEEE Trans. Microwave Theory Tech.*, vol. MTT-23, pp. 788–794, Oct. 1975.

[7] S. W. Yun and T. Itoh, "Nonreciprocal wave propagation in a hollow image guide with ferrite layer," *Proc. Inst. Elect. Eng.*, pt. H, vol. 132, no. 4, pp. 222–227, July 1985.

[8] P. Kwan and C. Vittoria, "Propagation characteristics of a ferrite image guide," *J. Appl. Phys.*, vol. 73, no. 10, pp. 6466–6469, May 1993.

[9] ——, "Scattering parameters measurement of a nonreciprocal coupling structure," *IEEE Trans. Microwave Theory Tech.*, vol. 41, pp. 652–657, Apr. 1993.

[10] ——, "Analysis of coupled magneto-dielectric image guides," *IEEE Trans. Magn.*, vol. 29, pp. 3425–3427, Nov. 1993.

[11] I. Awai and T. Itoh, "Coupled-mode theory analysis of distributed nonreciprocal structures," *IEEE Trans. Microwave Theory Tech.*, vol. MTT-29, pp. 1079–1086, Oct. 1981.

[12] T. J. Gerson and J. S. Nadan, "Surface electromagnetic modes of a ferrite slab," *IEEE Trans. Microwave Theory Tech.*, vol. MTT-22, pp. 757–762, Aug. 1974.

[13] D. M. Pozar, *Microwave Engineering*, 2nd ed. New York: Wiley, 1998.

Ahmet Soydan Akyol (S'02) was born in Malatya, Turkey, in 1974. He received the B.Sc. degree in electrical engineering and electronics from the Middle East Technical University, Ankara, Turkey, in 1996, the M.Sc. (Eng.) degree in electrical engineering and electronics from The University of Leeds, Leeds, U.K., in 1997, and the Ph.D. degree in microwave engineering from the University of Manchester Institute of Science and Technology (UMIST), Manchester, U.K., in 2002.

He is currently a Research and Development Engineer with ASELSAN A.S., Ankara, Turkey. His research interests include waveguide theory, nonreciprocal media, ferrites, microstrip ring resonators, antennas, and polarizers.

Dr. Akyol was a Student Paper Award Semifinalist at the 2001 IEEE Microwave Theory and Techniques Society (IEEE MTT-S) International Symposium (IMS), Phoenix, AZ. He was also the recipient of IEEE and UMIST traveling scholarships, a British Council-Turkish Education Foundation (TEV) Scholarship, and UMIST Graduate and Microwave Research Scholarships.

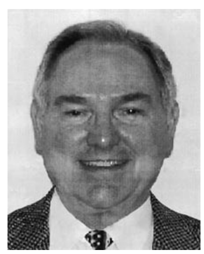

Lionel Edward Davis (SM'64–LF'95) received the B.Sc. (Eng.) degree from the University of Nottingham, Nottingham, U.K., and the Ph.D. and D.Sc. (Eng.) degrees from University College London, London, U.K.

From 1959 to 1964, he was with Mullard Research Laboratories, Redhill, U.K. From 1964 to 1972, he was a faculty member with the Electrical Engineering Department, Rice University, Houston, TX. From 1972 to 1987, he was with Paisley College, Paisley, Scotland, where he was Professor and Head of the Department of Electrical and Electronic Engineering. In 1987, he joined the Department of Electrical Engineering and Electronics, University of Manchester Institute of Science and Technology (UMIST), Manchester, U.K., where he is currently Professor of communication engineering and Head of the Microwave Engineering Group. He has been a Visiting Professor with the University College London and the University of California at San Diego, and has been a consultant for several companies. He has carried out research on passive components, high-T_c superconductors, dielectric-resonator antennas, chiral materials, and liquid crystal films. His current research interests are in gyrotropic media and nonreciprocal components for microwave, millimeter-wave, and optical wavelengths.

Dr. Davis is a Fellow of the Institution of Electrical Engineers (IEE), U.K., and of the Institute of Physics. He is a member of the IEEE Microwave Theory and Techniques Society (IEEE MTT-S) International Microwave Symposium (IMS) Technical Programme Committee, and co-chairman of the IEEE MTT-S Committee on Microwave Ferrites. Until recently, he was a member of the Administrative Committee of the UKRI MTT/AP/ED/LEOS chapter, and he initiated the Houston chapter of the IEEE MTT-S. He served on the Council, the Microwave Theory and Devices Committee, and the Accreditation Committee of the IEE and is member of the Peer Review College of the U.K. Engineering and Physical Sciences Research Council (EPSRC).